Quantum Electronics **50** (2) 169–174 (2020)

https://doi.org/10.1070/QEL17149

Efficiency enhancement of thermonuclear DD reaction in femtosecond laser plasma with the use of structured low-average-density targets

K.A. Ivanov, S.A. Shulyapov, I.N. Tsymbalov, A.A. Akunets, N.G. Borisenko,I.M. Mordvintsev, I.V. Bozh'ev, R.V. Volkov, S.G. Bochkarev, V.Yu. Bychenkov, A.B. Savel'ev

Abstract. **An increase in the yield of fast neutrons is experimentally demonstrated by exciting a nuclear DD reaction in the interaction of a relativistically intense (over 10^{18} W cm^{-2}) ultrashort laser pulse with a deuterated low-average-density target volume-structured at the wavelength scale. It is shown that decreasing the average target density from 0.78 to 0.35 g cm^{-3} doubles the neutron flux, which reaches 7×10^4 particles per 1 J of input energy. The effect may be associated with an increase in the number of accelerated deuterium ions due to the three dimensional expansion of individual elements of the target structure.**

Keywords: *relativistic laser plasma, thermonuclear DD reaction, neutron source, structured target.*

1. Introduction

Interaction of ultrashort laser pulses at peak radiation intensities above 10^{18} W cm^{-2} results in the production of relativistic laser plasma (see papers [1–3] and references therein). During laser irradiation, the electrons produced as a result of ionisation even at the pulse front gain an energy of up to several tens of MeV due to several acceleration mechanisms in the plasma layer of density slightly lower than the critical one. Penetrating into the bulk of the target, the charged particles generate bremsstrahlung X-ray radiation with a broad spectrum up to photon energies of several MeV. The same electrons form a quasi-static charge separation field at the interface, which accelerates ions to a high energy. The action of laser-accelerated particles onto the matter gives rise to different radiation/radioactive products, which are widely used in fundamental and applied problems [1]. These include, for instance, the production of a neutron source for the fundamental problems of materials science and the investigation of radiation resistance of materials, proton and neutron radiography, development of neutron detectors, etc. [4–7]. It is precisely the problem of laser-driven neutron generation that underlies the importance of our work.

Two approaches to neutron production in the high-intensity laser-plasma interaction can be pointed out to date. In the first one, laser-plasma products (gamma photons, protons) are used to excite a reaction resulting in a neutron yield [8–15]. In this case, usually close to the main (laser) target a secondary (nuclear) target is placed, which absorbs the accelerated particle flux from the plasma. Typically, nuclear reactions have a threshold of several MeV. The spectrum of resultant neutrons ranges from thermal (a fraction of an eV) to fast (above 1 MeV) ones. The second method most often implies laser irradiation of a target substance in which accelerated nuclei are produced and there are target nuclei. This, for example, is achieved with the use of a deuterated matter (or a deuterium–tritium target) [16–19]. In the resultant plasma, deuterium ions collide, and a fusion reaction occurs (DD-reaction with the formation of a ^{3}He nucleus and a neutron), which gives rise to a fast (2.45 MeV) neutron. We emphasise that in the former case the neutron flux is lower but its directivity is higher. In the latter case, the number of neutrons is much greater and their initial energy exceeds several MeV, but their expansion is almost isotropic [17].

On the whole, the average neutron flux obtained with the schemes described above is low in comparison with other types of neutron sources. However, the advantage of a laser neutron source is its high peak brightness, small source size, and short neutron pulse duration. To date, in the framework of the second neutron generation scheme, the record for laser systems with a Joule energy level in an ultrashort pulse has been reached in Ref. [19], where the output of more than 10^6 neutrons per 1 J of input energy per shot was measured at a peak radiation intensity approaching 10^{20} W cm^{-2}. This was achieved when a high-contrast (better than 10^{-12}) femtosecond pulse irradiated a bulk-heated low-density target in the form of deuterated plastic (CD_2) nanorods onto the surface. In this case, the structures are not dispersed by prepulses by the instance of arrival of the main pulse, unlike the case of longer

K.A. Ivanov, I.M. Mordvintsev, A.B. Savel'ev Faculty of Physics, Lomonosov Moscow State University, Vorob'evy Gory, 119991 Moscow, Russia; Lebedev Physical Institute, Russian Academy of Sciences, Leninsky prosp. 53, 119991 Moscow, Russia; e-mail: akvonavi@gmail.com;
S.A. Shulyapov, R.V. Volkov Faculty of Physics, Lomonosov Moscow State University, Vorob'evy Gory, 119991 Moscow, Russia;
I.N. Tsymbalov International Laser Centre, Lomonosov Moscow State University, Vorob'evy Gory, 119991 Moscow, Russia; Institute for Nuclear Research, Russian Academy of Sciences, prosp. 60-letiya Oktyabrya 7a, Moscow, Russia;
A.A. Akunets, N.G. Borisenko Lebedev Physical Institute, Russian Academy of Sciences, Leninsky prosp. 53, 119991 Moscow, Russia;
I.V. Bozh'ev Faculty of Physics and Centre of Quantum Technologies, Lomonosov Moscow State University, Vorob'evy Gory, 119991 Moscow, Russia;
S.G. Bochkarev, V.Yu. Bychenkov Lebedev Physical Institute, Russian Academy of Sciences, Leninsky prosp. 53, 119991 Moscow, Russia; Centre for Fundamental and Applied Research, Dukhov Automatics Research Institute (VNIIA), Sushchevskaya ul. 22, 127055 Moscow, Russia; e-mail: bochkar@lebedev.ru

Received 3 October 2019; revision received 20 November 2019
Kvantovaya Elektronika **50** (2) 169–174 (2020)
Translated by E.N. Ragozin

low-contrast pulses [16], and the radiation is not absorbed in the resultant preplasma away from the surface of the main target.

The matter is that, unlike the ordinary smooth target surface, when the laser pulse is absorbed in a thin skin layer at the surface, in the case of a micro- or nanostructured target it is possible to realise the regime of strong volume absorption with a high average target density. In this case, the efficiency of fusion reaction depends directly on the density and number of particles involved in the interaction. Furthermore, the regime of microstructures expanding under heating permits producing high-density plasma of extremely high temperature, which is also important for the efficiency of nuclear reaction process.

Similar effects are possible in the high-contrast pulsed irradiation of aerogels and other micro- and nanodimensionally structured targets (clusters and carbon nanotubes, as well as surface micro- and nanostructures on plane targets, including ordered and random submicron protuberances in the form of fibres, cones, spheres, grooves, holes, etc.). With such targets it is possible to achieve deep penetration of laser radiation into the target with an average density which may be as high as ~10% of the solid density.

Investigations of the application of volume-structured targets have long been pursued (see, for instance, Refs [20–22]), including from the standpoint of neutron generation [16, 23, 24]. Here, there is good reason to emphasise an important circumstance which shows to the best advantage the method of neutron production with deuterated targets as compared to the secondary target approach and, as a rule, high-power laser systems. The point is that the DD fusion reaction proceeds efficiently even at an ion temperature of about 100 keV, the reaction cross section peaking at a temperature of about 1 MeV [25]. This suggests that there is no need to use expensive and cumbersome sub-and petawatt laser systems to create a neutron source, whereas it is possible to do with more compact lasers that can generate pulses with a high repetition rate and thereby provide a high average neutron flux. At the same time, in Ref. [16] the maximum neutron yield from a plastic CD_2 target exposed to low contrast (10^{-4}) picosecond radiation corresponded to the yield from a bulk-homogeneous film with the maximum density, and for volume-structured samples the neutron yield decreased with a decrease in the average density.

Apart from the target structure, a significant effect on the characteristics of accelerated particles and secondary nuclear reaction products is exerted by the parameters of the laser pulse itself. Specifically, contrast of laser radiation may have a strong effect on the efficiency of ion acceleration (including deuterons). The presence of a prepulse ahead of the main laser pulse gives rise to a preplasma, in which the ion-accelerating ambipolar field become weaker [26–28]. However, the existence of a long subcritical-density preplasma may also lead to a growth of absorption and the consequential rise in the temperature and density of hot electrons, with the result that the efficiency of ion acceleration may become higher [29, 30]. Therefore, the influence of laser-plasma interaction conditions on the generation of neutron fluxes is also being investigated [28].

The present investigation is concerned with neutron production by DD fusion reaction under femtosecond pulsed laser irradiation of CD_2 targets of different average density, which are structured at a sub-wavelength scale, at a peak intensity of over 10^{18} W cm^{-2}. It is shown that neutron flux from the plasma attains a peak figure of 7×10^4 neutron J^{-1} pulse^{-1}. In this case, the average neutron yield is approximately two times higher in the irradiation of the target with a two-fold lower (0.35 versus 0.78 g cm^{-3}) density. In parallel, we observed a weak effect of the laser pulse contrast (used here were pulses with a contrast ratio of 10^{-8} and better than 10^{-9} as regards the pedestal formed by the amplified spontaneous luminescence) on the neutron yield from the targets employed in our work.

2. Experimental facility

Our experiments were performed using the radiation of a Ti : sapphire laser system (τ = 50 fs, λ = 805 nm, ν = 10 Hz). The on-target energy (up to 30 mJ) was monitored in each pulse with the use of a calibrated photodiode. The experiment is schematised in Fig. 1a. Inside the vacuum chamber the radiation was focused to spot ~4 μm in diameter (FWHM) employing an off-axis parabolic mirror. This provided a peak intensity of $\sim 2 \times 10^{18}$ W cm^{-2} for a 45° incidence angle on the target (a compromise value between the highest absorption for a sharp plasma–vacuum boundary at an incidence angle of ~60° and a lowering of the peak intensity with increasing incidence angle). The targets were made using a deuterated polymer: $(CD_2)_n$ polyethylene with deuteration degree of 97.5 at.%. A 50-mg powder sample was compressed at different forces (from 0.3 to 7.5 tons) with an exposure of about 5 min. The resultant targets were tablets 20 and 12 mm in diameter of density 0.78 and 0.35 g cm^{-3}. Weighing them with torsion balance and measuring their geometrical dimen-

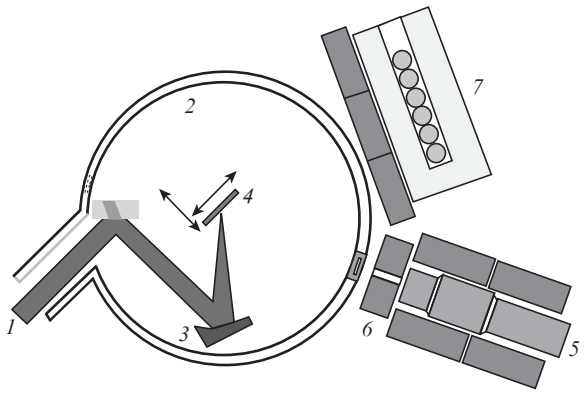

a

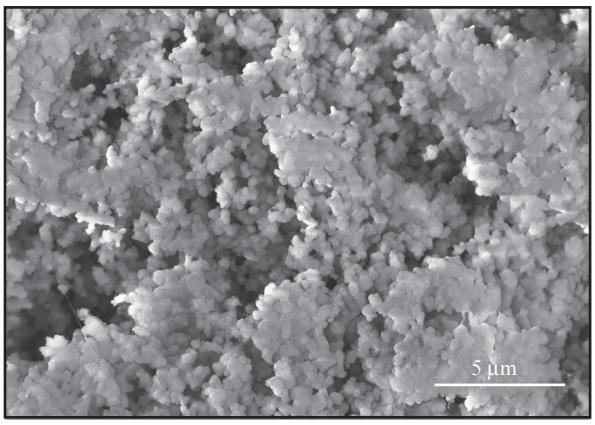

b

Figure 1. (a) Schematic of the experimental facility and (b) electron microscope image of the sample surface of average density 0.35 g cm^{-3}: (*1*) laser radiation; (*2*) vacuum chamber; (*3*) off-axis parabolic mirror; (*4*) target on motorised stages; (*5*) hard X-ray detector; (*6*) lead blocks; (*7*) moderator block with a ^{3}He-detector bundle.

sions with the use of an MBS-10 microscope provided a 3% uncertainty in determining the sample density. Figure 1b shows the surface image of the powder target of density 0.35 g cm^{-3} prior to pulsed laser irradiation, which was obtained employing a Zeiss Supra-40 electron microscope. One can see the characteristic surface inhomogeneity, the existence of nanostructures and caverns, which the sharply focused radiation can penetrate in. The number of such caverns is smaller in the samples of higher average density. Plane deuterated film of density $\sim$1 g cm^{-3} was also used as a reference test in studies of the spectrum of fast ions from the plasma.

The laser pulse contrast measured with respect to the pedestal of amplified spontaneous emission (ASE) was varied in our experiments. For an ordinary pulse the intensity contrast ratio was equal to $\sim 10^{-8}$ 10 ps ahead of the peak of the main pulse. On engaging the Cross Polarised Wave (XPW) [31] contrast cleaning system the contrast ratio became higher than 10^{-9}.

To diagnose the plasma, we used an X-ray scintillation detector designed to record the 100 keV – 10 MeV range photons. It was equipped with a system of lead blocks and shields for filtering and stopping the X-ray beam. The detector readings permitted estimating the 'quality' of a shot, i.e. the laser-to-hard X-ray energy conversion efficiency. This quantity provides a fairly objective assessment of the production efficiency of fast electrons, and they in turn determine to a large degree the acceleration of ions.

To detect neutrons, a set of ^{3}He counters was placed in the immediate vicinity of the vacuum chamber. The counters were surrounded by an acetylene moderator, which covered about 20% of the total solid angle. The signal was recorded in a time window of 1 ms using a digital oscilloscope with a bandpass of 250 MHz. The neutron production time in the plasma is determined by the electron-to-ion energy transfer time and amounts to several picoseconds. To estimate the efficiency of the neutron count system, instead of the target we placed a californium neutron source with a known activity. It emitted neutrons with an energy of $\sim$2 MeV, which is close to the energy of neutrons produced in the DD fusion reaction in the plasma. According to our measurements, the detector operated at a rate of 150 ± 30 Hz for an average Cf source decay rate of about 3×10^4 per second, which corresponds to a neutron detection efficiency of 0.5 ± 0.1% of the neutrons emanating from the plasma into the total solid angle.

The ion plasma spectrum was studied using the time-of-flight ion detection technique [26]. The statistics was accumulated in a series of several thousand shots. Next, proceeding from X-ray data, we excluded the shots that were unaccompanied by signals for one reason or another. It is noteworthy that the neutron detection statistics was Poissonian and depended little on the integral yield of hard X-rays (see below). Supposedly, this is an indication that the neutron yield depends more likely on the input laser energy and only slightly on the peak intensity in one or other laser pulse.

3. Main results

To estimate the ion spectrum in the plasma, at first we address the ion diagnostics data. Figure 2 shows the deuteron spectrum measured for a target in the form of a plane deuterated CD_2 film for a laser pulse contrast ratio of 10^{-8}. In the case of metal targets, this contrast ratio results in the formation of a thin preplasma layer with a characteristic length of several tenths of the wavelength along the target normal [32]. For transparent dielectric targets, this contrast would be sufficiently high to prevent the plasma production by a prepulse. It counts in favour of the assumption that the structures of the powder samples are not eroded by the instant of arrival of the main pulse. One can see that the ion energy (E) distribution in the $E \gtrsim 100$ keV domain is close to the exponentially decaying one with an effective spectrum 'temperature' of about 120 keV. Since the ion temperature in the plasma is proportional to the hot electron energy, the latter may also be estimated at 120–150 keV. Under the assumption of mainly the ponderomotive electron acceleration/heating under the interaction conditions, this figure is in reasonable agreement with our earlier simulation data [33]. Our measurements cannot provide information about the deuteron spectrum at energies below 10–20 keV and there is no way to study their contribution to the thermonuclear fusion reaction, although this problem is topical for elucidating the cross sections for low-energy nuclear reactions. Nevertheless, considering the extremely small reaction cross section in the range $E < 10$ keV (below 10^{-31} m^2, Fig. 2) [25], the main contribution to neutron production under our experimental conditions is made by deuterons with energies of 50–200 keV.

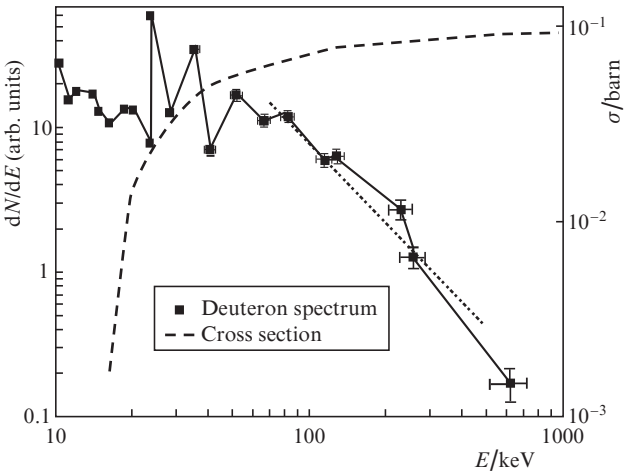

Figure 2. Deuteron in the laser plasma at the CD_2 film and cross section for the DD fusion with neutron production; the dotted line approximates the spectrum by an exponentially decaying function with an effective temperature $T = 120 \pm 20$ keV.

As noted above, the detected neutron number correlates only slightly with the amplitude of the X-ray detector signal (Fig. 3a). In this case, the neutron signal was absent for those laser pulses which generated no X-rays. It is possible to estimate the average number of neutrons generated per pulse by summing the number of neutrons detected in about one thousand laser pulses. For the higher-density sample (0.78 g cm^{-3}) and the pulse with a contrast ratio of 10^{-8}, this quantity turned out to be equal to 0.58 ± 0.15 neutrons per pulse, or about 100 neutrons per pulse into the total solid angle, taking into account the detector efficiency and the isotropic neutron distribution [17]. Nevertheless, the relatively strong pulse-to-pulse scatter of neutron yield data, to all appearances, is indication that the radiation fortunately finds its way into a cavern, dent, or other structural irregularity on the target. The data on the average neutron yield are, on the whole, similar to

our earlier results for the ordinary film. It is therefore valid to say that the pressed target of density ~0.8 g cm^{-3} is little different from the solid film. The highest detected yield was equal to 5 neutrons per pulse, or about 3×10^4 per one Joule of laser energy. The laser pulse that produced the highest recorded neutron yield was not accompanied by a huge X-ray detector signal, which additionally bears out the statistical independence of the two data sets.

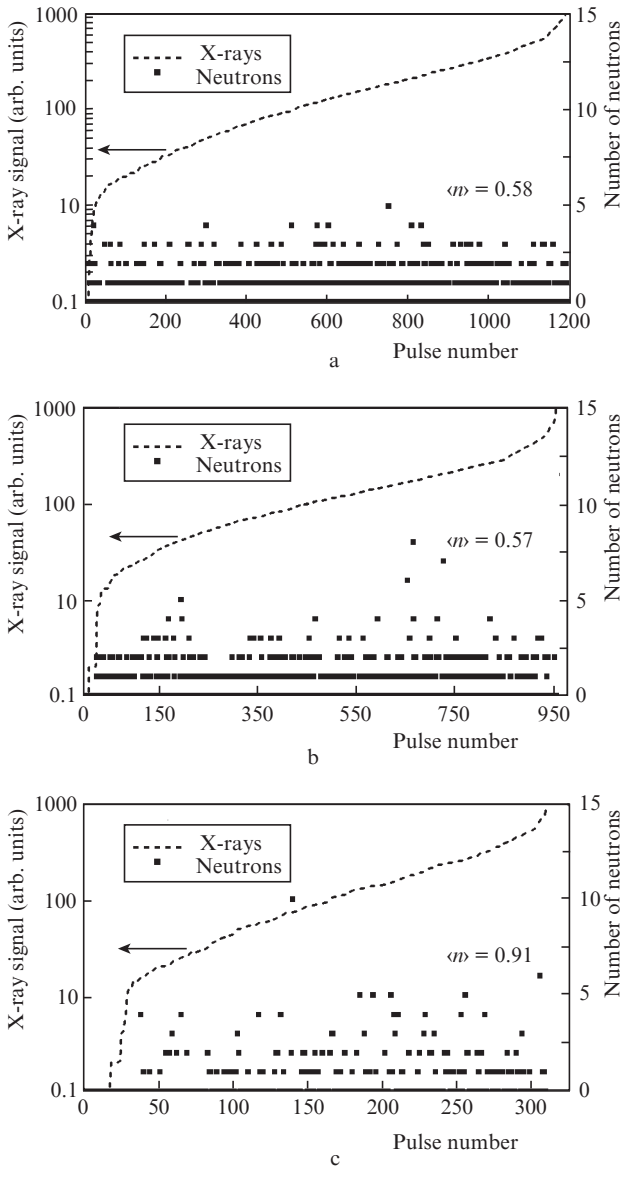

Figure 3. Amplitude of X-ray detector signals in each laser pulse and number of detected neutrons in the same pulse for (a, b) a target with an average density of 0.78 g cm^{-3} and a pulse contrast of (a) 10^{-8} and (b) higher than 10^{-9} as well as for (c) a target with an average density of 0.35 g cm^{-3} and a pulse contrast ratio of 10^{-8}; $\langle n \rangle$ is the number of neutrons per pulse averaged over the entire series of measurements.

The appearance of so large a number of neutrons in an individual laser pulse cannot be attributed to the statistics of our measurements. The point is that, for a nearly simultaneous detection of all neutrons in some laser pulse (in a time window of 500 μs), the determining role is played not by the photocount statistics (which was significant in the neutron measurements from the test source) but the statistics of neutron exit angle distribution, i.e. the neutron spatial distribution statistics. This distribution is isotropic in our conditions. For an average number of 100 neutrons per pulse and a total detection angle of 0.8π (20% of the total solid angle), the detector records 20 events. According to the Poissonian statistics, the probability of detecting 10 times more particles is negligible in this case and cannot manifest itself even in a sample of 1000 laser shots. Specifically, even if we do not take into account the detector efficiency and proceed from the average number of ~0.5 neutrons per pulse, the probability of detecting 5 neutrons in some pulse is equal to ~10^{-4}, i.e. only 0.1 in 1000 pulses. Therefore, the efficiency of DD-reaction excitation does show a rather strong pulse-to-pulse scatter, which may be attributed to the strong inhomogeneity of the target surface.

The estimated average yield of 3×10^4 neutrons per 1 Joule is in reasonable agreement with the data of other scientific groups that operated with similar intensities of femtosecond laser radiation. For a longer pulse of the picosecond range, the yield turns out to be higher by an order of magnitude [16], which may be related to a more efficient ion acceleration into the target interior (ions are accelerated when the pulse still persists, the accelerating potential lasts longer). With increasing laser energy, the efficiency of neutron flux production will certainly increase due to the growth of the population of fast (or so-called hot) electrons (from a fraction of percent to several percent [34]). These electrons largely determine the number of deuterons accelerated to high (above 10 keV) energies, which can enter into the fusion reaction.

Going over to the pulse with a higher contrast ratio (better than 10^{-9}) did entail a noticeable change in the neutron yield from the plasma (Fig. 3b). This is another indication that a contrast ration of 10^{-8} is already sufficient to provide the interaction of the main ultrashort laser pulse with the weakly perturbed initial structured surface. The average yield is also at a level of 0.57 neutrons per pulse in a series of thousand pulses. It is believed that a higher contrast of laser pulses results in electron acceleration at a sharper target boundary and, as a consequence, a stronger ion-accelerating ambipolar field [26]. However, it is so when electrons which are flying away from target are considered and not which are going into it. In our case, the decisive role is supposedly played by the target surface morphology. The penetration of radiation between the structures is responsible for the three-dimensional local expansion of the target material, which is accompanied by the production of a large plasma volume with a high average ion energy. An improvement of proton and deuteron acceleration efficiency was demonstrated experimentally also for microstructured 'snow' targets with large-scale formations [35] as well as for nanocolumns in Refs [19, 36].

The deuteron density in the plasma that enter the fusion reaction may be easily estimated proceeding from the average number of detected neutrons. Fast ions, like hot electrons, are produced in the domain of peak absorption of laser radiation. According to SRIM data [37], for particles of energy ~100 keV the average particle absorption length d measures ~1 μm in the CD_2 material of density 0.78 g cm^{-3}. In view of the average DD reaction cross section $\sigma \approx 0.07$ barn in the 50–200 keV energy range and a deuterium atom density $n_d \approx 0.7 \times 10^{23}$ cm^{-3} (for a substance density of 0.78 g cm^{-3}), it is possible to estimate the reaction probability $P_{DD} = d\sigma n_d \approx$

5×10^{-7}. Since the average number of neutrons in the total solid angle is equal to $\sim 10^2$ per pulse, the total number of fast deuterium ions is simply defined as the ratio of the number of generated neutrons to the probability P_{DD}, i.e. amounts to $\sim 2 \times 10^8$. Then, the energy conversion efficiency of laser pulses to high-energy ions (with an average energy of 100 keV) is estimated at $\sim 10^{-4}$.

In our case, the pulsed laser irradiation of the lower density (0.35 g cm^{-3}) target was noted for a statistically valid, nearly two-fold (up to 0.91 ± 0.2) increase in the average number of neutrons per pulse in comparison with the higher density sample (Fig. 3c). In the most successful shot, the neutron yield may be estimated at $\sim 7 \times 10^4$ per 1 J of laser energy. This result is indicative of the trend opposite to the previously observed one in Ref. [16], where the neutron yield decreased in the irradiation of a low-density target by a low-contrast pulse.

Proceeding from the surface structure it may be assumed that the growth of the number of neutrons is due to a more frequent entry of pulses into caverns on the target, which are the sites of three-dimensional expansion of the hot plasma. It is therefore valid to emphasise the promising use of structured targets, where each pulse of the laser system irradiates a prepared target area. To this end, of course, the sample fabrication and the irradiation area should be carefully monitored, but this task is technically quite realisable. Of course, numerical simulations are required to elucidate the cause of the effect observed. Our results nevertheless show the promise of investigations with low-density targets in the regime of ultrashort high-contrast irradiation. Of course, these estimates should be made more accurate, since one can expect not only the effect of an increased volume of hot plasma. The results of more detailed numerical simulations and analytical calculations, as well as of experiments with other targets, will be published elsewhere.

4. Conclusions

In the course of our investigation we showed the way of increasing the yield of neutrons produced by the DD fusion reaction in the laser plasma on the surface of a deuterated target. Specifically, for a deuterated polyethylene target with a structured surface and an average density of ~ 0.35 g cm^{-3} exposed to laser irradiation with a peak intensity of $\sim 2 \times 10^{18}$ W cm^{-2}, the peak neutron yield to the total solid angle amounted to 7×10^4 per 1 J of laser energy. This is two times greater than in the irradiation of a similar target of higher density (0.78 g cm^{-3}) under similar experimental conditions. Simple estimates and an analysis of the surface images of the samples suggest that the observed effect may be attributed to the volume absorption of laser radiation in the caverns and dents on the target surface. For the target with a lower average density, the surface turns out to be more friable, with the effect that the radiation 'fortunately' finds its way into these irregularities more often.

As mentioned above, the goal of modern investigations is to improve the neutron yield without increasing the energy of a laser pulse; otherwise, this entails a significant increase in the size of the facility itself. The goal is to make a compact neutron source, and specially prepared targets show promise for this purpose. The use of a structured target with a low average density is advantageous in the first place in that it permits achieving to a greater extent the regime of volume radiation absorption, when the number of particles involved in acceleration process will be much larger even despite the lowering of the overall target density. Furthermore, when the target structure comprises dense domains of size comparable with the laser irradiation wavelength, their expansion under heating would be directed not only away from or into the bulk of the target, but also towards other expanding domains, which increases the number of collisions.

We emphasise that laser systems similar to the one we use may be upgraded in the future for obtaining a high pulse repetition rate [38], which is important in the development of new radioactive sources, including a compact neutron source.

Our result indicates the high potentiality of specially prepared targets from the standpoint of development of compact laser-plasma neutron sources. Research in this direction will be continued, and it is highly likely that the neutron yield will further increase with the use of targets having parameters preliminarily simulated numerically and calculated analytically.

Acknowledgements. This work was supported by the Russian Science Foundation (Grant No. 17-12-01283). The time-of-flight spectrometer was prepared and adjusted in the framework of Grant No. 18-32-00416 from the Russian Foundation for Basic Research. The authors express their gratitude to A.N. Paskhalov and N.V. Eremin for placing at their disposal the neutron detector and the calibration source. The electron microscopy of the target surface was performed using the equipment of the Educational and Methodical Centre of Lithography and Microscopy, Lomonosov Moscow State University.

References

1. Ledingham K.W.D., Galster W. *New J. Phys*., **12**, 045005 (2010).
2. Daido H., Nishiuchi M., Pirozhkov A.S. *Rep. Prog. Phys*., **75**, 056401 (2012).
3. Galy J., Hamilton D.J., Normand C. *Eur. Phys. J. Spec. Top*., **175**, 147 (2009).
4. Alvarez J. et al. *Phys. Procedia*, **60**, 29 (2014).
5. Brenner C.M. et al. *Plasma Phys. Control. Fusion*, **58**, 014039 (2016).
6. Gerbaux M. et al. *Rev. Sci. Instrum*., **79**, 023504 (2008).
7. Kardjilov N. et al. *Materials Today*, **14**, 248 (2011).
8. Willingale L. et al. *Phys. Plasmas*, **18**, 083106 (2011).
9. Schwoerer H. et al. *Phys. Rev. Lett*., **86**, 2317 (2001).
10. Davis J., Petrov G.M. *Plasma Phys. Control. Fusion*, **50**, 065016 (2008).
11. Higginson D.P. et al. *Phys. Plasmas*, **18**, 100703 (2011).
12. Tsymbalov I.N. et al. *Yadernaya Fiz*., **80**, 1 (2017).
13. Giulietti D. et al. *Nucl. Instrum. Methods B*, **402**, 373 (2017).
14. Roth M. et al. *Phys. Rev. Lett*., **110**, 044802 (2013).
15. Krasa J. et al. *High Pow. Las. Sci. Engin*., **2**, e19 (2014).
16. Belyaev V.D. et al. *J. Phys. IV France*, **133**, 507 (2006).
17. Demchenko N.N. et al. *JETP*, **128**, 178 (2019) [*Zh. Eksp. Teor. Fiz*., **155**, 204 (2019)].
18. Satoh N. et al. *Plasma Fus. Res*., **13**, 2401028 (2018).
19. Curtis A. et al. *Nature Commun*., **9**, 1077 (2018).
20. Murnane M.M., Falcone H.C. *Appl. Phys. Lett*., **62**, 1068 (1993).
21. Volkov R.V. et al. *Quantum Electron*., **28**, 1 (1998) [*Kvantovaya Elektron*., **25**, 3 (1998)].
22. Kulcsar G. et al. *Phys. Rev. Lett.,* **84**, 5149 (2000).
23. Volkov R.V. et al. *JETP Lett*., **72**, 401 (2000) [*Pis'ma Zh. Eksp. Teor. Fiz*., **72**, 577 (2000)].
24. Golishnikov D.M. et al. *Laser Phys*., **11**, 1205 (2001).
25. https://www-nds.iaea.org/exfor/endf.htm.
26. Shulyapov S.A. et al. *Quantum Electron*., **46**, 432 (2016) [*Kvantovaya Elektron*., **46**, 432 (2016)].

27. Flacco A. et al. *Nucl. Instrum. Methods A*, **620**, 18 (2010).
28. Varmazyar P. et al. *Laser Part. Beams*, **36**, 226 (2018).
29. McKenna P. et al. *Laser Part. Beams*, **26**, 591 (2008).
30. Sentoku Y. et al. *Appl. Phys. B*, **74**, 207 (2002).
31. Jullien A. et al. *Opt. Lett*., **30**, 920 (2005).
32. Ivanov K.A. et al. *Phys. Plasmas*, **24**, 063109 (2017).
33. Tsymbalov I. et al. *Plasma Phys. Control. Fusion*, **61**, 075016 (2019).
34. Beg F. et al. *Phys. Plasmas*, **4**, 447 (1997).
35. Ziegler A. et al. *Phys. Rev. Lett*., **110**, 215004 (2013).
36. Dozières M. et al. *Plasma Phys. Control. Fusion*, **61**, 065016 (2019).
37. Ziegler J. *SRIM & TRIM* (2017); http://www.srim.org/.
38. Hah J. et al. *Plasma Phys. Control. Fusion*, **60**, 054011 (2018).